Channel state information estimation for 5G wireless communication systems: Recurrent neural networks approach

Mohamed Hassan Ali [Corresp., 1] , **Ibrahim B. M. Taha** [2]

[1] Department of Electrical Engineering, Faculty of Engineering, Al-Azhar University,, 1Department of Electrical Engineering, Faculty of Engineering, Al-Azhar University, Qena 83513, Egypt, Qena, Qena, Egypt

[2] Department of Electrical Engineering, College of Engineering,, Taif University, Taif 21944,, Saudi Arabia, Taif, Taif

Corresponding Author: Mohamed Hassan Ali
Email address: mhessai@azhar.edu.eg

In this study, a deep learning bidirectional long short-term memory (BiLSTM) recurrent neural network-based channel state information estimator is proposed for 5G orthogonal frequency-division multiplexing systems. The proposed estimator is a pilot-dependent estimator and follows the online learning approach in the training phase and the offline approach in the practical implementation phase. The estimator does not deal with complete a priory certainty for channels' statistics and attains superior performance in the presence of a limited number of pilots. A comparative study is conducted using three loss functions, namely, mean absolute error, cross entropy function for kth mutually exclusive classes and sum of squared of the errors. The Adam optimisation algorithm is used to evaluate the performance of the proposed estimator under each loss function. In terms of symbol error rate and accuracy metrics, the proposed estimator outperforms long short-term memory (LSTM) neural network-based channel state information, least squares and minimum mean square error estimators under different simulation conditions. The computational and training time complexities for deep learning BiLSTM- and LSTM-based estimators are provided. Given that the proposed estimator relies on the deep learning neural network approach, where it can analyse massive data, recognise statistical dependencies and characteristics, develop relationships between features and generalise the accrued knowledge for new datasets that it has not seen before, the approach is promising for any 5G and beyond communication system.

Channel State Information Estimation for 5G Wireless Communication Systems: Recurrent Neural Networks Approach

Mohamed Hassan Essai Ali[1] and Ibrahim B. M. Taha[2]

[1]Department of Electrical Engineering, Faculty of Engineering, Al-Azhar University, Qena 83513, Egypt
[2]Department of Electrical Engineering, College of Engineering, Taif University, Taif 21944, Saudi Arabia

Corresponding Author:
Mohamed Hassan Essai Ali [1]
Masaken Osman, Qena, Qena, 83513, Egypt
Email address: mhessai@azhar.edu.eg

Abstract

In this study, a deep learning bidirectional long short-term memory (BiLSTM) recurrent neural network-based channel state information estimator is proposed for 5G orthogonal frequency-division multiplexing systems. The proposed estimator is a pilot-dependent estimator and follows the online learning approach in the training phase and the offline approach in the practical implementation phase. The estimator does not deal with complete a priory certainty for channels' statistics and attains superior performance in the presence of a limited number of pilots. A comparative study is conducted using three loss functions, namely, mean absolute error, cross entropy function for kth mutually exclusive classes and sum of squared of the errors. The Adam optimisation algorithm is used to evaluate the performance of the proposed estimator under each loss function. In terms of symbol error rate and accuracy metrics, the proposed estimator outperforms long short-term memory (LSTM) neural network-based channel state information, least squares and minimum mean square error estimators under different simulation conditions. The computational and training time complexities for deep learning BiLSTM- and LSTM-based estimators are provided. Given that the proposed estimator relies on the deep learning neural network approach, where it can analyse massive data, recognise statistical dependencies and characteristics, develop relationships between features and generalise the accrued knowledge for new datasets that it has not seen before, the approach is promising for any 5G and beyond communication system.

Introduction

5G wireless communication is the most active area of technology development and a rapidly growing branch of the wider field of communication systems. Wireless communication has made possible various services ranging from voice to multimedia.

The physical characteristics of the wireless communication channel and many unknown surrounding effects result in imperfections in the transmitted signals. The transmitted signals experience reflections, diffractions and scattering, which in turn produce multipath signals with different delays, phase shift, attenuation and distortion arriving at the receiving end; hence, they adversely affect the recovered signals.

A priori information on the physical characteristics of the channel provided by pilots is one of the major factors that determine the efficiency of channel state information estimators (CSIEs). For instance, if not a priori information is available (no or insufficient pilots), then channel estimation is useless; finding what you do not know is impossible. When complete information on the transmission channel is available, CSIEs are no longer needed. Thus, a priori uncertainty exists for communication channel statistics. However, the classical theory of detection, recognition and estimation of signals deals with complete a priory certainty for channel statistics, and it is an unreliable and unpractical assumption.

In the classic case, uncertainty is related to useful signals. In detection problems, the unknown is the fact of a signal existence. In recognition problems, the unknown is the type of signal being received at the current moment. In estimation problems, the unknown is the amplitude of the measured signal or one of its parameters. The rest of the components of the signal-noise environment in classical theory are regarded as a priori certain (known) as follows: the known is the statistical description of the noise, the known is the values of the unmeasured parameters of the signal and the known is the physical characteristics of the wireless communication channel. In such conditions, the classical theory allows the synthesis of optimal estimation algorithms, but the structure and quality coefficients of the algorithms depend on the values of the parameters of the signal-noise environment. If the values of the parameters describing the signal-noise environment are slightly different from the parameters for which the optimal algorithm is built, then the quality coefficients will become substantially poor, making the algorithm useless in several cases [1], [2].

The most frequently used CSIEs are derived from signal and channel statistical models by employing techniques, such as maximum likelihood (ML), least squares (LS) and minimum mean squared error (MMSE) optimisation metrics [3].

One of the major concerns in the optimum performance of wireless communication systems is the means of providing accurate channel state information (CSI) at the receiver end of the systems to coherently detect the transmitted signal. If CSI is unavailable at the receiver end, then the transmitted signal can only be demodulated and detected by a noncoherent technique, such as differential demodulation. However, the use of a noncoherent detection method occurs at the expense of a loss of signal-to-noise ratio of about 3–4 dB compared with using a coherent detection technique. To eliminate such losses, researchers have focused on the development of channel estimation techniques to provide perfect detection of transmitted information in wireless communication systems using the OFDM modulation scheme [4].

The use of deep learning neural networks (DLNNs) is the state-of-the-art approach in the field of wireless communication. The amazing learning capabilities of DLNNs from training data sets and the tremendous progress of graphical processing units (GPUs), which are considered the most powerful tools for training DLNNs, have motivated its usage for different wireless communication issues, such as modulation recognition [5], [6] and channel state estimation and detection [7-13]. According to [4] – [7] and [10], all proposed deep learning-based CSIEs have better performance compared with the examined traditional channel ones, such as LS and MMSE estimators.

Recently, numerous long short-term memory (LSTM)- and BiLSTM-based applications have been introduced for prognostic and health management [14], artificial intelligence-based translation systems [15], [16] and other areas.

For channel state information estimation in 5G-OFDM wireless communication systems, many deep learning approaches, such as convolutional neural network (CNN), recurrent neural network (RNN) (e.g. LSTM and BiLSTM NNs) and hybrid (CNN and RNN) neural networks have been used.

In [17], a deep learning-based CSIE was proposed by using CNN and BiLSTM-NN for the extraction of the feature vectors of the channel response and channel estimation, respectively. The aim was to improve the channel state information estimation performance at the downlink, which is caused by the fast time-varying and varying channel statistical characteristics in high-speed mobility scenarios. In [18], an online-trained CSIE that is an integration of CNN and LSTM-NN was proposed. The authors also developed an offline–online training technique that applies to 5G wireless communication systems. In [7], a joint channel estimator and detector that is based on feedforward DLNNs for frequency selective channel (OFDM) systems was introduced. The proposed algorithm was found to be superior to the traditional MMSE estimation method when unknown surrounding effects of communication systems are considered. In [19], an online estimator was developed by adopting feedforward DLNNs for doubly selective channels. The proposed estimator was considered superior to the traditional LMMSE estimator in all investigated scenarios. In [10], a one-dimensional CNN (1D-CNN) deep learning estimator was proposed. Under various modulation scenarios and in terms of MSE and BER metrics, the authors compared the performance of the proposed estimator with that of feedforward neural networks (FFNN), MMSE and LS estimators. 1D-CNN outperformed LS, MMSE and FFNN estimators. In [11], an online pilot-assisted estimator model for OFDM wireless communication systems was developed by using LSTM NN. The conducted comparative study showed the superior performance of the proposed estimator in comparison with LS and MMSE estimators under limited pilots and a prior uncertainty of channel statistics. The authors in [20] used the genetic algorithm-optimised artificial neural network to build a CSIE. The proposed estimator was dedicated for space–time block-coding MIMO-OFDM communication systems. The proposed estimator outperformed LS and MMSE estimators in terms of BER at high SNRs, but it achieved approximately the same performance as LS and MMSE estimators at low SNRs. The authors in [21] proposed a CSIE for OFDM systems by using ANN under the condition of sparse multipath channels. The proposed estimator achieved a comparable SER performance as matching pursuit- and orthogonal matching pursuit-based estimators at a lower computational complexity than that of the examined estimators.

In this study, a BiLSTM DLNN-based CSIE for OFDM wireless communication systems is proposed and implemented. To the best of the authors' knowledge, this work is the first to use the BiLSTM network as a CSIE without integration with CNN. The proposed estimator does not need any prior knowledge of the communication channel statistics and powerfully works at limited pilots (under the condition of less CSI).

Although an impressively wide range of configurations can be found for almost every aspect of deep neural networks, one element is underrepresented when addressing communication problems: most studies and applications simply use the 'log' loss function [22].

The loss function estimates the loss between the expected and actual outcome. This function can be calculated in many ways. Selecting a loss function is one of the essential and challenging tasks in deep learning. During the learning process, optimisation (learning) algorithms try to minimise the available loss function to the desired error goal by optimising the DLNN weights and biases iteratively at each training epoch. The proposed estimator is trained using the Adam optimisation algorithm and three different loss functions to obtain the most optimal BiLSTM-based estimator for wireless communication systems with low prior information (limited pilots) for signal-noise environments. The obtained results show that the BiLSTM-based estimator attains a comparable performance as the MMSE estimator and outperforms LS and MMSE estimators at large and small numbers of pilots, respectively. In addition, the proposed estimator improves the transmission data rate of OFDM wireless communication systems because it exhibits optimal performance compared with the examined estimators at a small number of pilots.

The proposed BiLSTM-based CSIE is a data-driven estimator, so it can analyse, recognise and understand the statistical characteristics of wireless channels suffering from many known and

unknown interferences. The performance of the proposed BiLSTM-based estimator is compared with the performance of the most frequently used LS and MMSE channel state estimators.

The rest of this paper is organised as follows. The DLNN-based CSIE is presented in Section II. The standard OFDM system and the proposed deep learning BiLSTM NN-based CSIE are presented in Section III. The simulation results are given in Section IV. The conclusions and future work directions are provided in Section V.

DLNN-BASED CSIE

Add your materials and methods here.

In this section, a deep learning BiLSTM NN for channel state information estimation is presented. The BiLSTM network is another version of LSTM neural networks, which are recurrent neural networks (RNN) that can learn the long-term dependencies between the time steps of input data [23] [14, 24].

The BiLSTM architecture mainly consists of two separate LSTM-NNs and has two propagation directions (forward and backward). The LSTM NN structure consists of input, output and forget gates and a memory cell. The forget and input gates enable the LSTM NN to effectively store long-term memory. Figure 1 shows the main construction of the LSTM cell. The forget gate enables LSTM NN to remove the undesired information by currently used input x_t and cell output h_t of the last process. The input gate finds the information that will be used with the previous LSTM cell state c_{t-1} to obtain a new cell state c_t based on the current cell input x_t and the previous cell output h_{t-1}. Using the forget and input gates, LSTM can decide which information is abandoned and which is retained.

The output gate finds current cell output h_t by using the previous cell output h_{t-1} at current cell state c_t and input x_t. The mathematical model of the LSTMNN structure can be described through Equations (1)–(6).

$$i_t = \sigma_g\left(w_i x_t + R_i h_{t-1} + b_i\right), \quad (1)$$

$$f_t = \sigma_g\left(w_f x_t + R_f h_{t-1} + b_f\right), \quad (2)$$

$$g_t = \sigma_c\left(w_g x_t + R_g h_{t-1} + b_g\right), \quad (3)$$

$$o_t = \sigma_g\left(w_o x_t + R_o h_{t-1} + b_o\right), \quad (4)$$

$$c_t = f_t \odot c_{t-1} + i_t \odot g_t, \quad (5)$$

$$h_t = o_t \odot \sigma_c(c_t), \quad (6)$$

where i, f, g, o, σ_c, σ_g and $\odot$ denote the input gate, forget gate, cell candidate, output gate, state activation function (hyperbolic tangent function (tanh), gate activation function (sigmoid function) and Hadamard product (element-wise multiplication of vectors), respectively. $\mathbf{W} = [w_i \; w_f \; w_g \; w_o]^T$, $\mathbf{R} = [R_i \; R_f \; R_g \; R_o]^T$ and $\mathbf{b} = [b_i \; b_f \; b_g \; b_o]^T$ are input weights, recurrent weights and bias, respectively.

The forward and backward propagation directions of BiLSTM are transmitted at the same time to the output unit. Therefore, old and future information can be captured, as shown in Figure 2. At any time t, the input is fed to forward LSTM and backward LSTM networks. The final output of BiLSTM-NN can be expressed as follows:

$$h_t = \overrightarrow{h_t} \odot \overleftarrow{h_t}, \quad (7)$$

where $\overrightarrow{h_t}$ and $\overleftarrow{h_t}$ are forward and backward outputs of BiLSTM-NN, respectively.

The proposed BiLSTM-based CSIE is built. The weights and biases of the proposed estimator are optimised (tuned) using the Adam optimization algorithm. Adam trains the proposed estimator by using three loss functions, namely, mean absolute error (MAE), cross entropy function for k^{th} mutually exclusive classes (crossentropyex) and sum of squared errors (SSE). The use of these loss functions aims to obtain the most reliable and robust estimator under unknown channel statistical characteristics and limited pilot numbers.

To build the DL BiLSTM NN-based CSIE, an array is created with the following five layers: sequence input, BiLSTM, fully connected, softmax and output classification. The input size was set to 256. The BiLSTM layer consists of 16 hidden units and shows the sequence's last element. Four classes are specified by considering the size 4 fully connected (FC) layer, followed by a softmax layer and ended by a classification layer. Figure 3(a) illustrates the structure of the proposed estimator. Figure 3(a) can be compacted in one block as in Figure 3(b).

DL BiLSTM NN-BASED CSIE for 5G–OFDM WIRELESS COMMUNICATION SYSTEMS

The standard OFDM wireless communication system and an offline DL of the proposed CSIE are presented in the following subsections.

OFDM SYSTEM MODEL

In accordance with [11], Figure 4 clearly illustrates the structure of the traditional OFDM communication system.On the transmitter side, a serial-to-parallel converter is used to convert the transmitted symbols with pilot signals into parallel data streams. Then, inverse discrete Fourier transform is applied to convert the signal into the time domain. A cyclic prefix must be added to alleviate the effects of inter-symbol interference. The length of the cyclic prefix must be longer than the maximum spreading delay of the channel.

The multipath channel of a sample space defined by complex random variables $\{h(n)\}_{n=0}^{N-1}$ is considered. Then, the received signal can be evaluated as follows:

$$y(n) = x(n) \oplus h(n) + w(n), \qquad (8)$$

where $x(n)$ is the input signal, $\oplus$ is circular convolution, $w(n)$ is additive white Gaussian noise (AWGN) and $y(n)$ is the output signal.

The received signal in the frequency domain can be defined as

$$Y(k) = X(k)H(k) + W(k), \qquad (9)$$

where the discrete Fourier transformations of $x(n)$, $h(n)$, $y(n)$ and $w(n)$ are $X(k)$, $H(k)$, $Y(k)$ and $W(k)$, respectively. These discrete Fourier transformations are estimated after removing CP. The OFDM frame includes the pilot symbols of the 1st OFDM block and the transmitted data of the next OFDM blocks. The channel can be considered stationary during a certain frame, but it can change between different frames. The proposed DL BiLSTM NN-based CSIE receives the arrived data at its input terminal and extracts the transmitted data at its output terminal [11], [7].

OFFLINE DL OF THE DL BILSTM NN-BASED CSIE

DLNN utilisation is the state-of-the-art approach in the field of wireless communication, but DLNNs have high computational complexity and long training time. GPUs are the most powerful tools used for training DLNNs [25]. Training should be done offline due to the long training time of the proposed CSIE and the large number of BILSTM-NN's parameters, such as biases and weights, that should be tuned during training. The trained CSIE is then used in online implementation to extract the transmitted data [7], [11].

In offline training, the learning dataset is randomly generated for one subcarrier. The transmitting end sends OFDM frames to the receiving end through the adopted (simulated) channel, where each frame consists of single OFDM pilot symbol and a single OFDM data symbol. The received OFDM signal is extracted based on OFDM frames that are subjected to different channel imperfections.

All classical estimators rely highly on tractable mathematical channel models, which are assumed to be linear, stationary and follow Gaussian statistics. However, practical wireless communication systems have other imperfections and unknown surrounding effects that cannot be tackled well by accurate channel models; therefore, researchers have developed various channel models that effectively characterise practical channel statistics. By using these channel models, reliable and practical training datasets can be obtained by modelling [1], [11], [26].

In this study, the 3GPP TR38.901-5G channel model developed by [26] is used to simulate the behaviour of a practical wireless channel that can degrade the performance of CSIEs and hence, the overall communication system's performance.

The proposed estimator is trained via Adam optimisation, which updates the weights and biases by minimising a specific loss function. Simply, a loss function is defined as the difference between the estimator's responses and the original transmitted data. The loss function can be represented by several functions. MATLAB/software allows the user to choose a loss function amongst its available list that contains crossentropyex, MSE, sigmoid and softmax. In this study, another two custom loss functions (MAE and SSE) are created. The performance of the proposed estimator when using three loss functions (i.e. MAE, crossentropyex and SSE) is investigated. The loss functions can be expressed as follows:

$$crossentropyex = -\sum_{i=1}^{N}\sum_{j=1}^{c} X_{ij}(k)\log(\hat{X}_{ij}(k)), \tag{10}$$

$$MAE = \frac{\sum_{i=1}^{N}\sum_{j=1}^{c}\left|X_{ij}(k)-\hat{X}_{ij}(k)\right|}{N}, \tag{11}$$

$$SSE = \sum_{i=1}^{N}\sum_{j=1}^{c}\left(X_{ij}(k)-\hat{X}_{ij}(k)\right)^2, \tag{12}$$

where N is the sample number, c is the class number, X_{ij} is the i^{th} transmitted data sample for the j^{th} class and $\hat{}$ is the DL BiLSTM-based CSIE response for sample i for class j.

Figure 5 illustrates the processes of generating the training data sets and offline DL to obtain a learned CSIE based on BiLSTM-NN.

Simulation Results

STUDYING THE PERFORMANCE OF THE PROPOSED, LS AND MMSE ESTIMATORS BY USING DIFFERENT PILOTS AND LOSS FUNCTIONS

Several simulation experiments are performed to evaluate the performance of the proposed estimator. In terms of symbol error rate (SER) performance analysis, the SER performance of the proposed estimator under various SNRs is compared with that of the LSTM NN-based CSIE [11], the well-known LS estimator and the MMSE estimator, which is an optimal estimator but requires channel statistical information. A priori uncertainty of the used channel model statistics is assumed and considered for all conducted experiments.

Moreover, the Adam optimisation algorithm is used to train the proposed estimator whilst using different loss functions to obtain the most robust version of the proposed CSIE. The proposed model is implemented in 2019b MATLAB/software.

Table 1 lists the parameters of BiLSTM-NN and LSTM-NN architectures and their related training options. These parameters are identified by a trial-and-error approach. Table 2 lists the parameters of the OFDM system model and the channel model.

The examined estimators' performance is evaluated at different pilot numbers of 4, 8 and 64 as well as crossentropyex, MAE and SSE loss functions. The Adam optimisation algorithm is used for all simulation experiments.

With a sufficiently large number of pilots (64) and the use of the crossentropyex loss function, the proposed $\text{BiLSTM}_{\text{crossentropyex}}$ estimator outperforms $\text{LSTM}_{\text{crossentropyex}}$, LS and MMSE estimators over the entire SNR range, as shown in Figure 6.

Figure 7 indicates that at pilot number = 64 and with the MAE loss function, the $BiLSTM_{MAE}$ estimator outperforms the LS estimator over the SNR range [0–18 dB], but $LSTM_{MAE}$ outperforms it over the SNR range [0–15 dB]. In addition, the $BiLSTM_{MAE}$ and $LSTM_{MAE}$ estimators are at par with the MMSE estimator over the SNR ranges [0–10 dB] and [0–4 dB], respectively. Beyond these SNR ranges, the MMSE estimator outperforms $BiLSTM_{MAE}$ and $LSTM_{MAE}$ estimators. BiLSTMMAE outperforms $LSTM_{MAE}$ starting from 5 dB to 20 dB.

At the same number of pilots and with the use of the SSE loss function, Figure 8 shows that the $BiLSTM_{SSE}$ and $LSTM_{SSE}$ estimators achieve the same performance as the MMSE estimator over a low SNR range [0–7 dB]. MMSE outperforms the $BiLSTM_{SSE}$ and $LSTM_{SSE}$ estimators starting from 8 dB, and the LS estimator outperforms $BiLSTM_{SSE}$ starting from 15 dB and $LSTM_{SSE}$ starting from 13 dB. $BiLSTM_{SSE}$ outperforms $LSTM_{SSE}$ starting from 9 dB to 20 dB. LS provides poor performance compared with MMSE because it does not use prior information about channel statistics in the estimation process. MMSE exhibits superior performance, especially with sufficient pilot numbers, because it uses second-order channel statistics.

Figure 9 summarises the performance of the proposed and the other considered estimators for various loss functions at 64 pilots. MMSE and the proposed $BiLSTM_{crossentropyex}$ attain close SER performance with respect to all SNRs. Furthermore, at low SNR (0–7 dB), $BiLSTM_{(crossentropyex,\ MAE,\ and\ SSE)}$, $LSTM_{(crossentropyex,\ MAE,\ and\ SSE)}$ and MMSE attain approximately the same performance.

Figures 10–13 present the performance comparison of LS, MMSE, BiLSTM and LSTM-based estimators using the Adam optimisation algorithm and the different (crossentropyex, MAE and SSE) loss functions at 8 pilots. Figure 13 shows that the proposed $BiLSTM_{(crossentropyex,\ or\ MAE\ or\ SSE)}$ estimators outperform the $LSTM_{(crossentropyex,\ or\ MAE\ or\ SSE)}$ estimators and the traditional estimators over the examined SNR range. At a low SNR (0–7 dB), the proposed $BiLSTM_{(crossentropyex,\ or\ MAE\ or\ SSE)}$ estimators exhibit identical performance. Furthermore, the proposed $BiLSTM_{SSE}$ estimator trained by minimising the SSE loss function outperforms the $BiLSTM_{crossentropyex}$ estimator trained by minimising the crossentropyex loss function starting from 8 dB; it outperforms $BiLSTM_{MAE}$, which is trained by minimising the MAE loss function starting from 16 dB.

Figures 14–17 show the performance comparison of the LS, MMSE, $BiLSTM_{(crossentropyex,\ or\ MAE\ or\ SSE)}$ and $LSTM_{(crossentropyex,\ or\ MAE\ or\ SSE)}$ estimators at 4 pilots. Figure 17 shows the superiority of the proposed $BiLSTM_{(crossentropyex,\ or\ MAE\ or\ SSE)}$ estimators in comparison with the traditional estimators, which have lost their workability starting from 0 dB. It also shows the superiority of the proposed estimator $BiLSTM_{(MAE\ or\ SSE)}$ over $LSTM_{(MAE\ or\ SSE)}$. $LSTM_{(crossentropyex)}$ exhibits a competitive performance as $BiLSTM_{(crossentropyex)}$ starting from 0 dB to 12 dB, and $LSTM_{(crossentropyex)}$ outperforms $BiLSTM_{(crossentropyex)}$ starting from 13 dB.

At very low SNRs (0–3 dB), the proposed $BiLSTM_{(crossentropyex,\ or\ MAE\ or\ SSE)}$ estimators have the same performance. The proposed $BiLSTM_{SSE}$ estimator outperforms the $BiLSTM_{crossentropyex}$ estimator starting from 4 dB, and it exhibits an identical performance as the $BiLSTM_{MAE}$ estimator until 14 dB and outperforms it in the rest of the SNR examination range.

Figures 13, 17 and 18 emphasise the robustness of the BiLSTM-based estimators against the limited number of pilots and under the condition of a priori uncertainty of channel statistics. They demonstrate the importance of testing various loss functions in the deep learning process to obtain the most optimal architecture of any proposed estimator.

Figure 18 indicates that the proposed $BiLSTM_{crossentropyex}$, $BiLSTM_{SSE}$ and $BiLSTM_{SSE}$ estimators have close SER performance at 64, 8 and 4 pilots, respectively. The performance of $BiLSTM_{SSE}$ at 8 pilots coincides with the performance of $BiLSTM_{crossentropyex}$ at 64 pilots. Therefore, using the proposed estimators with few pilots is recommended for 5G OFDM wireless communication systems to attain a significant improvement in their transmission data rate. Given that the proposed estimator adopts a training data set-driven approach, it is robust to a priori uncertainty for channel statistics.

LOSS CURVES

The quality of the DLNNs' training process can be monitored efficiently by exploring the training loss curves. These loss curves provide information on how the training process goes, and the user can decide whether to let the training process continue or stop.

Figures 19–21 show the loss curves of the DLNN-based estimators (BiLSTM and LSTM) at pilot numbers = 64, 8 and 4 and with the three examined loss functions (crossentropyex, MAE and SSE). The curves emphasise and verify the obtained results in Figure 6 through Figure 17. For example, the sub-curves in Figure 19 for $\text{BiLSTM}_{\text{crossentropyex}}$ and $\text{LSTM}_{\text{crossentropyex}}$ estimators emphasise their superiority over the other estimators. This superiority can be seen clearly from Figures 9. Moreover, the training loss curves in Figures 20 and 21 emphasise the obtained SER performance in Figures 13 and 17, respectively, of each examined DLNN-based CSIE.

ACCURACY CALCULATION

The accuracy of the proposed and other examined estimators is a measure of how the estimators recover transmitted data correctly. Accuracy can be defined as the number of correctly received symbols divided by the total number of transmitted symbols. The proposed estimator is trained in different conditions as indicated in the previous subsection, and we wish to investigate how well it performs in a new data set. Tables 3, 4 and 5 present the obtained accuracies for all examined estimators under all simulation conditions.

As illustrated in Tables 3 to 5, the proposed BiLSTM-based estimator attains accuracies from 98.61 to 100 under different pilots and loss functions. The other examined DL LSTM-based estimator has accuracies from 97.88 to 99.99 under the same examination conditions. The achieved accuracies indicate that the proposed estimator has robustly learned and emphasises the obtained SER performance in Figure 18. The obtained results of MMSE and LS in Tables 1, 2 and 3 emphasise the presented SER performance in Figures 9, 13 and 17, respectively, and show that as the pilot number decreases, the accuracy of the conventional estimators dramatically decreases.

The proposed BiLSTM- and LSTM-based estimators rely on DLNN approaches, where they can analyse huge data sets that may be collected from any plant, recognise the statistical dependencies and characteristics, devise the relationships between features and generalise the accrued knowledge for new data sets that they have not seen before. Thus, they are applicable to any 5G and beyond communication system.

COMPLEXITY

The feed-forward pass and feed-back pass operations dominate the computational complexity $O(W)$ of all neural networks, such as FFNNs, LSTM and BiLSTM. In a feed-forward pass, the weighted sum of inputs from previous layers to the next layers is calculated. In feed-back pass, the errors are evaluated; hence, the weights are modified.

The computational complexity of LSTM is

$$O(W) = O(KH + KCS + HI + CSI), \qquad (13)$$

where W is the weight number, K is the output unit number, H is the hidden unit number, I is the input number, C is the memory cell block number and S is the memory cell block size [23].

The BiLSTM architecture has two separate LSTM-NNs and two propagation directions (forward and backward). Hence, for BiLSTM, $W = 2W$. The computational complexity of BiLSTM is

$$O(2W) = O(2(KH + KCS + HI + CSI)). \qquad (14)$$

The required training time can be used as another a complexity metric. Table 6 lists the consumed processing time for the examined BiLSTM- and LSTM-based CSIEs. The used computer is equipped with an Intel(R) Core (TM) i5-2400 CPU running with a 3.10–3.30 GHz microprocessor and 4 GB of RAM. The LSTM-based estimators consume less processing time than the BiLSTM-based estimators do. Hence, they have the lowest complexity.

CONCLUSIONS

We summarise the paper by listing the main conclusions in separate points, as follows:

i. The proposed DL-BiLSTM-based CSIE is an online pilot assisted estimator. It is robust against a limited number of pilots and exhibits superior performance compared with conventional estimators.
ii. The proposed CSIE is robust under the conditions of a priori uncertainty of communication channel statistics (non-Gaussian/stationary statistical channels) and demonstrates superior performance compared with conventional estimators and DL LSTM NN-based CSIEs.
iii. The proposed CSIE exhibits a consistent performance at large and small pilot numbers and superior performance at low SNRs, especially at limited pilots, compared with conventional estimators.
iv. The proposed CSIE achieves the highest accuracy amongst all examined estimators at 64, 8 and 4 pilots for all the used loss functions.
v. The proposed BiLSTM- and LSTM-based estimators have high prediction accuracies of 98.61% to 100% and 97.88% to 99.99%, respectively, when using crossentropyex, MAE and SSE loss functions for 64, 8 and 4 pilots. They are promising for 5G and beyond wireless communication systems.
vi. Two customised loss functions (MAE and SSE) are introduced.
vii. The computational and training time complexities are presented to illustrate the complexity of the proposed estimator compared with that of the LSTM-based estimator.

FUTURE WORK

i. Investigating the proposed estimator's performance and accuracy by using other learning algorithms, such as Adadelta, Adagrad, AMSgrad, AdaMax and Nadam.
ii. Investigating the proposed estimator's performance and accuracy by using different cyclic prefix lengths and types.
iii. Developing robust loss functions by using robust statistics estimators, such as Tukey, Cauchy, Huber and Welsh.
iv. Investigating the performance of CNN-, gated recurrent unit (GRU)- and simple recurrent unit (SRU)-based CSIEs whilst using crossentropyex, MAE and SSE loss functions and for 64, 8 and 4 pilots.

Acknowledgements

The authors would like to acknowledge the financial support received from Taif University Researchers Supporting Project Number (TURSP-2020/61), Taif University, Taif, Saudi Arabia.

References

[1] V. Bogdanovich, A. J. J. o. C. T. Vostretsov, and Electronics, "Application of the invariance and robustness principles in the development of demodulation algorithms for wideband communications systems," vol. 54, no. 11, pp. 1283-1291, 2009.
[2] T. O'Shea, K. Karra, and T. C. Clancy, "Learning approximate neural estimators for wireless channel state information," in 2017 IEEE 27th international workshop on machine learning for signal processing (MLSP), 2017, pp. 1-7: IEEE.
[3] H. Kim, Wireless communications systems design. John Wiley & Sons, 2015.

[4] O. O. Oyerinde and S. H. Mneney, "Review of Channel Estimation for Wireless Communication Systems," IETE Technical Review, vol. 29, no. 4, pp. 282-298, 2012/07/01 2012.

[5] R. Zhou, F. Liu, and C. W. Gravelle, "Deep Learning for Modulation Recognition: A Survey With a Demonstration," IEEE Access, vol. 8, pp. 67366-67376, 2020.

[6] K. Karra, S. Kuzdeba, and J. Petersen, "Modulation recognition using hierarchical deep neural networks," in 2017 IEEE International Symposium on Dynamic Spectrum Access Networks (DySPAN), 2017, pp. 1-3.

[7] H. Ye, G. Y. Li, and B. Juang, "Power of Deep Learning for Channel Estimation and Signal Detection in OFDM Systems," IEEE Wireless Communications Letters, vol. 7, no. 1, pp. 114-117, 2018.

[8] Y. Yang, F. Gao, X. Ma, and S. Zhang, "Deep Learning-Based Channel Estimation for Doubly Selective Fading Channels," IEEE Access, vol. 7, pp. 36579-36589, 2019.

[9] X. Ma, H. Ye, and Y. Li, "Learning Assisted Estimation for Time- Varying Channels," in 2018 15th International Symposium on Wireless Communication Systems (ISWCS), 2018, pp. 1-5.

[10] S. Ponnaluru and S. Penke, "Deep learning for estimating the channel in orthogonal frequency division multiplexing systems," Journal of Ambient Intelligence and Humanized Computing, 2020/05/03 2020.

[11] M. H. Essai Ali, "Deep learning-based pilot-assisted channel state estimator for OFDM systems," IET Communications, vol. 15, no. 2, pp. 257-264, 17 January 2021.

[12] J. Joo, M. C. Park, D. S. Han, and V. J. I. A. Pejovic, "Deep learning-based channel prediction in realistic vehicular communications," IEEE Access, vol. 7, pp. 27846-27858, 2019 2019.

[13] J.-M. Kang, C.-J. Chun, and I.-M. J. I. A. Kim, "Deep Learning Based Channel Estimation for MIMO Systems With Received SNR Feedback," IEEE Access, vol. 8, pp. 121162-121181, 2020.

[14] C. Zhao, X. Huang, Y. Li, and M. J. S. Yousaf Iqbal, "A Double-Channel Hybrid Deep Neural Network Based on CNN and BiLSTM for Remaining Useful Life Prediction," vol. 20, no. 24, p. 7109, 2020.

[15] Y. Wu et al., "Google's neural machine translation system: Bridging the gap between human and machine translation," 2016.

[16] T. Ong, "Facebook's translations are now powered completely by AI," ed, 2017.

[17] Y. Liao, Y. Hua, X. Dai, H. Yao, and X. Yang, "ChanEstNet: A deep learning based channel estimation for high-speed scenarios," in ICC 2019-2019 IEEE International Conference on Communications (ICC), 2019, pp. 1-6: IEEE.

[18] C. Luo, J. Ji, Q. Wang, X. Chen, P. J. I. T. o. N. S. Li, and Engineering, "Channel state information prediction for 5G wireless communications: A deep learning approach," vol. 7, no. 1, pp. 227-236, 2018.

[19] Y. Yang, F. Gao, X. Ma, and S. J. I. A. Zhang, "Deep learning-based channel estimation for doubly selective fading channels," vol. 7, pp. 36579-36589, 2019.

[20] A. Sarwar, S. M. Shah, and I. Zafar, "Channel Estimation in Space Time Block Coded MIMO-OFDM System using Genetically Evolved Artificial Neural Network," in 2020 17th International Bhurban Conference on Applied Sciences and Technology (IBCAST), 2020, pp. 703-709: IEEE.

[21] H. Senol, A. R. B. Tahir, and A. J. T. S. Özmen, "Artificial neural network based estimation of sparse multipath channels in OFDM systems," Telecommunication Systems, pp. 1-10, 26 January 2021 2021.
[22] K. Janocha and W. M. J. a. p. a. Czarnecki, "On loss functions for deep neural networks in classification," 2017.
[23] S. Hochreiter and J. Schmidhuber, "Long Short-Term Memory," vol. 9, no. 8 %J Neural Comput., pp. 1735–1780, 1997.
[24] C. Luo, J. Ji, Q. Wang, X. Chen, P. J. I. T. o. N. S. Li, and Engineering, "Channel state information prediction for 5G wireless communications: A deep learning approach," 2018.
[25] R. Sharma, M. Vinutha, and M. Moharir, "Revolutionizing machine learning algorithms using gpus," in 2016 International Conference on Computation System and Information Technology for Sustainable Solutions (CSITSS), 2016, pp. 318-323: IEEE.
[26] "3GPP. TR38.901 Study on Channel Model for Frequencies from 0.5 to 100 GHz; 3GPP: Sophia Antipolis, France, 2019.," Technical report 2019 2019. 3rd gGeneration Partenership Project (3GPP), Technical Specification Group Radio Access Network

Figure 1

Long short-term memory (LSTM) cell.

II. DLNN-BASED CSIE

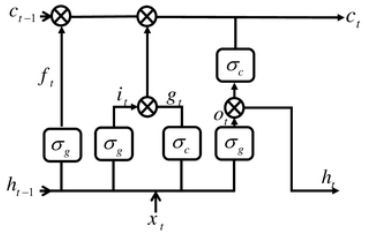

FIGURE 1. Long short-term memory (LSTM) cell.

Figure 2

BiLSTM-NN architecture.

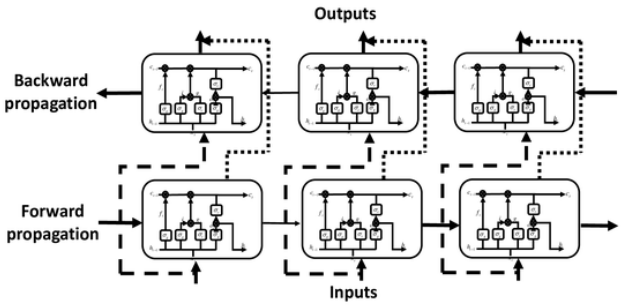

FIGURE 2. BiLSTM-NN architecture.

Figure 3

(a) Structure of the DL BiLSTM NN for the BiLSTM estimator and (b) compacted version of (a).

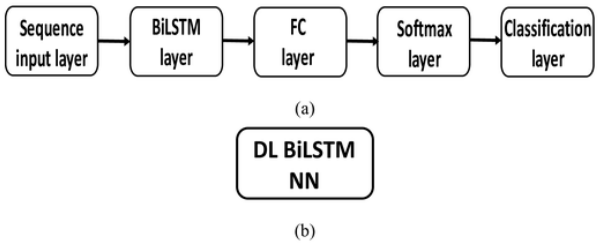

FIGURE 3. (a) Structure of the DL BiLSTM NN for the BiLSTM estimator and (b) compacted version of (a).

Figure 4

Conventional OFDM system

III. DL BiLSTM NN-BASED CSIE for 5G–OFDM WIRELESS COMMUNICATION SYSTEMS

A. OFDM SYSTEM MODEL

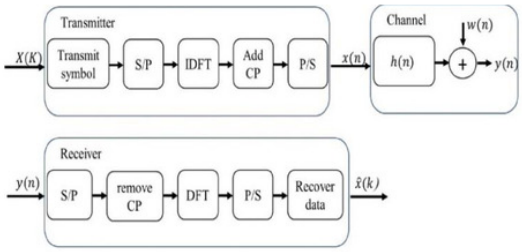

FIGURE 4. Conventional OFDM system [11].

Figure 5

Training data set formation and offline DL process of the BiLSTM-NN-based CSI estimator.

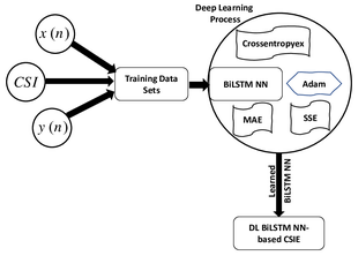

FIGURE 5. Training data set formation and offline DL process of the BiLSTM-NN-based CSI estimator.

Figure 6

SER comparison of the proposed, LSTM and conventional estimators using 64 pilots and the crossentropyex loss function.

IV. SIMULATION RESULTS

A. STUDYING THE PERFORMANCE OF THE PROPOSED, LS AND MMSE ESTIMATORS BY USING DIFFERENT PILOTS AND LOSS FUNCTIONS

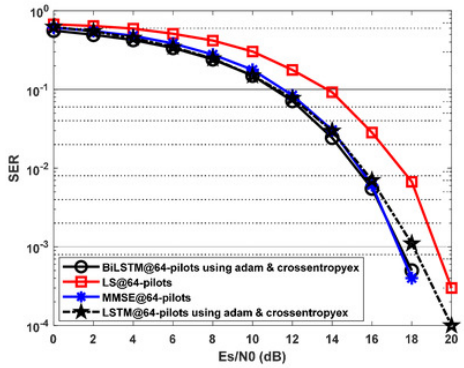

FIGURE 6. SER comparison of the proposed, LSTM and conventional estimators using 64 pilots and the crossentropyex loss function.

Figure 7

SER comparison of the proposed, LSTM and traditional estimators using 64 pilots and the MAE loss function.

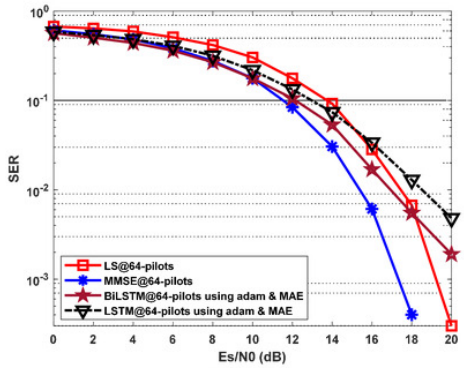

FIGURE 7. SER comparison of the proposed, LSTM and traditional estimators using 64 pilots and the MAE loss function.

Figure 8

SER comparison of the proposed, LSTM and traditional estimators using 64 pilots and the SSE loss function.

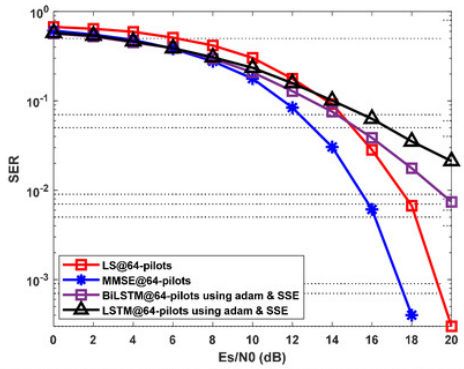

FIGURE 8. SER comparison of the proposed, LSTM and traditional estimators using 64 pilots and the SSE loss function.

Figure 9

SER comparison of LS, MMSE, BiLSTM and LSTM estimators using 64 pilots, the Adam learning algorithm and crossentropyex, MAE and SSE loss functions.

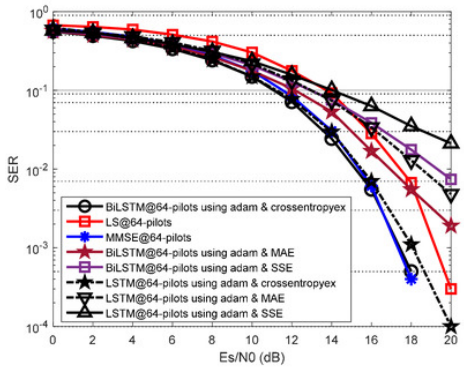

FIGURE 9. SER comparison of LS, MMSE, BiLSTM and LSTM estimators using 64 pilots, the Adam learning algorithm and crossentropyex, MAE and SSE loss functions.

Figure 10

SER performance comparison of the proposed, LSTM and conventional estimators using 8 pilots and the crossentropyex loss function.

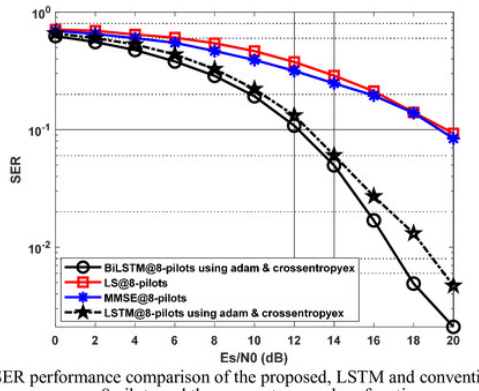

FIGURE 10. SER performance comparison of the proposed, LSTM and conventional estimators using 8 pilots and the crossentropyex loss function.

Figure 11

SER performance comparison of the proposed, LSTM and conventional estimators using 8 pilots and the MAE loss function.

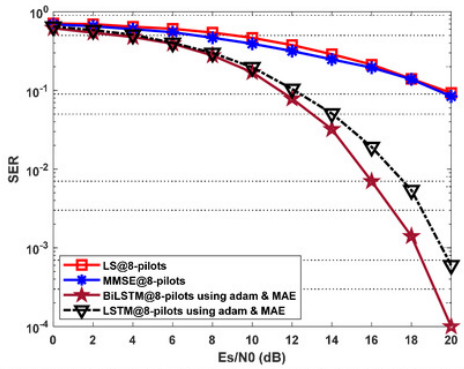

FIGURE 11. SER performance comparison of the proposed, LSTM and conventional estimators using 8 pilots and the MAE loss function.

Figure 12

SER performance comparison of the proposed, LSTM and conventional estimators using 8 pilots and the SSE loss function.

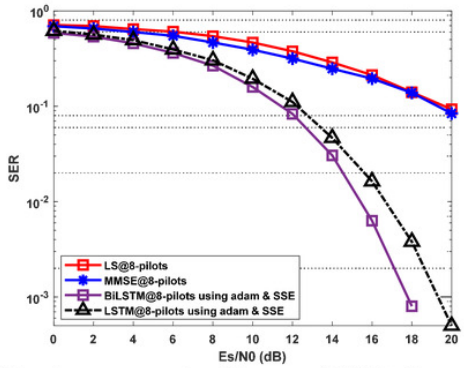

FIGURE 12. SER performance comparison of the proposed, LSTM and conventional estimators using 8 pilots and the SSE loss function.

Figure 13

SER performance comparison of LS, MMSE, LSTM and BiLSTM estimators using 8 pilots, the Adam learning algorithm and crossentropyex, MAE and SSE loss functions.

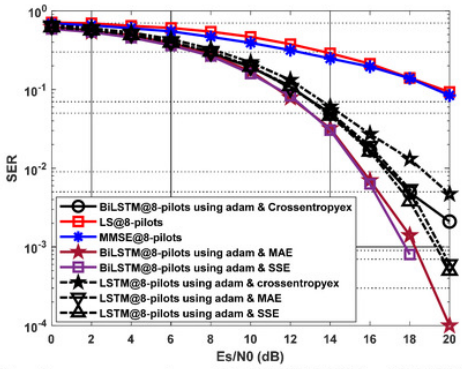

FIGURE 13. SER performance comparison of LS, MMSE, LSTM and BiLSTM estimators using 8 pilots, the Adam learning algorithm and crossentropyex, MAE and SSE loss functions.

Figure 14

SER performance comparison of the proposed, LSTM and conventional estimators using 4 pilots and the crossentropyex loss function.

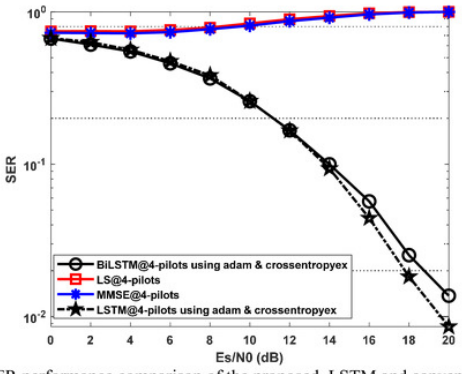

FIGURE 14. SER performance comparison of the proposed, LSTM and conventional estimators using 4 pilots and the crossentropyex loss function.

Figure 15

SER performance comparison of the proposed, LSTM and conventional estimators using 4 pilots and the MAE loss function.

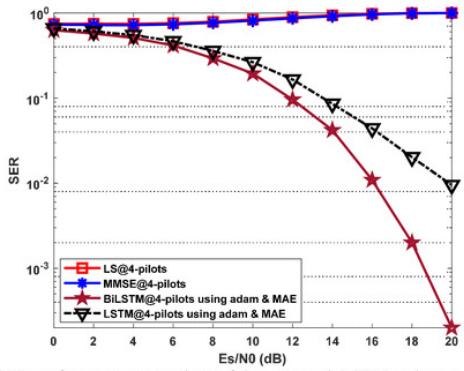

FIGURE 15. SER performance comparison of the proposed, LSTM and conventional estimators using 4 pilots and the MAE loss function.

Figure 16

SER performance comparison of the proposed, LSTM and conventional estimators using 4 pilots and the SSE loss function.

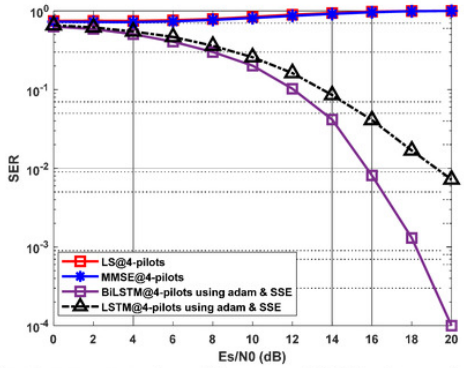

FIGURE 16. SER performance comparison of the proposed, LSTM and conventional estimators using 4 pilots and the SSE loss function.

Figure 17

SER performance comparison of LS, MMSE, LSTM and BiLSTM estimators using 4 pilots, the Adam learning algorithm and crossentropyex, MAE and SSE loss functions.

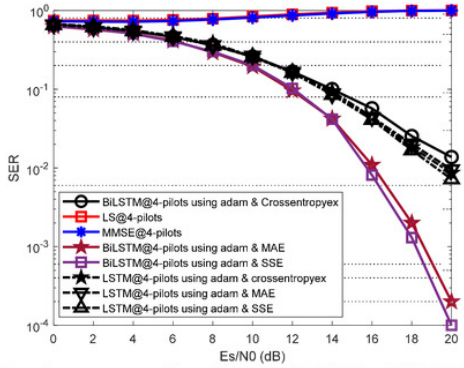

FIGURE 17. SER performance comparison of LS, MMSE, LSTM and BiLSTM estimators using 4 pilots, the Adam learning algorithm and crossentropyex, MAE and SSE loss functions.

Figure 18

SER performance comparison of the best DL BiLSTM-based CSIEs using various pilots and loss functions.

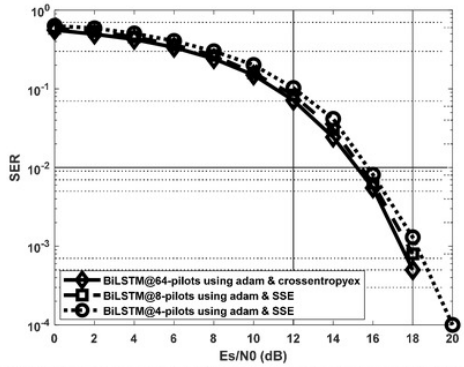

FIGURE 18. SER performance comparison of the best DL BiLSTM-based CSIEs using various pilots and loss functions.

Figure 19

Loss curves comparison of BiLSTM- and LSTM- based estimators using 64 pilots, the Adam learning algorithm and crossentropyex, MAE and SSE loss functions.

B. *LOSS CURVES*

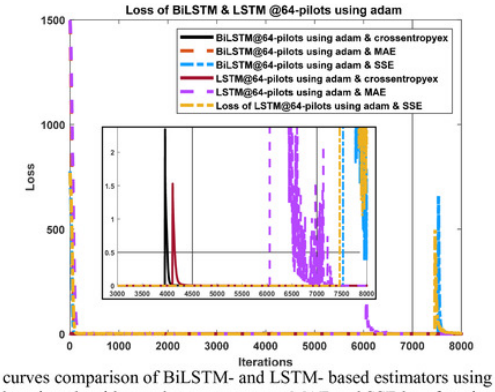

FIGURE 19. Loss curves comparison of BiLSTM- and LSTM- based estimators using 64 pilots, the Adam learning algorithm and crossentropyex, MAE and SSE loss functions.

Figure 20

Loss curves comparison of BiLSTM- and LSTM-based estimators using 8 pilots, the Adam learning algorithm and crossentropyex, MAE and SSE loss functions.

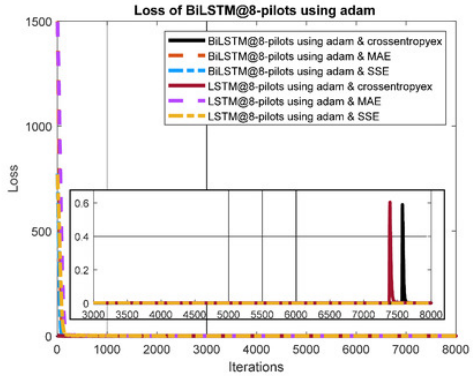

FIGURE 20. Loss curves comparison of BiLSTM- and LSTM-based estimators using 8 pilots, the Adam learning algorithm and crossentropyex, MAE and SSE loss functions.

Figure 21

Loss curves comparison of BiLSTM- and LSTM-based estimators using 4 pilots, the Adam learning algorithm and crossentropyex, MAE and SSE loss functions.

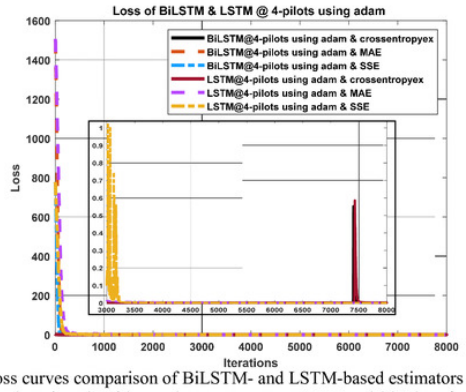

FIGURE 21. Loss curves comparison of BiLSTM- and LSTM-based estimators using 4 pilots, the Adam learning algorithm and crossentropyex, MAE and SSE loss functions.

Table 1(on next page)

BiLSTM- and LSTM-NN structure parameters and training process options

IV. SIMULATION RESULTS

A. STUDYING THE PERFORMANCE OF THE PROPOSED, LS AND MMSE ESTIMATORS BY USING DIFFERENT PILOTS AND LOSS FUNCTIONS

TABLE 1
BiLSTM- AND LSTM-NN STRUCTURE PARAMETERS AND TRAINING PROCESS OPTIONS

Parameter	Value
Input Size	256
BiLSTM Layer Size	30 hidden neurons
LSTM Layer Size	30 hidden neurons
FC Layer Size	4
Loss Functions	Crossentropyex, MAE, SSE
Mini Batch Size	1000
Epochs Number	1000
Learning Algorithm	Adam

Table 2(on next page)

OFDM system and channel parameters

TABLE 2
OFDM SYSTEM AND CHANNEL PARAMETERS

Parameter	Value
Modulation Mode	QPSK
Carrier Frequency	2.6 GHz
Paths Number	24
CP Length	16
Subcarrier Number	64
Pilot Number	64, 8 and 4

Table 3(on next page)

Accuracy comparison of the examined estimators using 64 pilots

B. ACCURACY CALCULATION

TABLE 3
ACCURACY COMPARISON OF THE EXAMINED ESTIMATORS USING 64 PILOTS

	64 pilots			
	BiLSTM	**LSTM**	**MMSE**	**LS**
Crossentropyex	100	99.99	100	99.94
SSE	99.23	97.88	100	99.96
MAE	99.87	99.52	100	99.97

Table 4(on next page)

Accuracy comparison of the examined estimators using 8 pilots

TABLE 4

ACCURACY COMPARISON OF THE EXAMINED ESTIMATORS USING 8 PILOTS

	8 pilots			
	BiLSTM	**LSTM**	**MMSE**	**LS**
Crossentropyex	99.84	99.53	91.34	91.62
SSE	100	99.95	91.60	91.49
MAE	100	99.94	91.53	91.50

Table 5(on next page)

Accuracy comparison of the examined estimators using 4 pilots

TABLE 5
ACCURACY COMPARISON OF THE EXAMINED ESTIMATORS USING 4 PILOTS

	4 pilots			
	BiLSTM	**LSTM**	**MMSE**	**LS**
Crossentropyex	98.61	97.94	0.24	0.02
SSE	100	99.28	0.24	0.09
MAE	99.97	99.05	0.26	0.04

Table 6(on next page)

Processing time comparison of the examined DLNN-based CSIEs

C. COMPLEXITY

TABLE 6
PROCESSING TIME COMPARISON OF THE EXAMINED DLNN-BASED CSIES

	64 pilots		8 pilots		4 pilots	
	Bi-LSTM	LSTM	Bi-LSTM	LSTM	Bi-LSTM	LSTM
Crossentropyex	10:13	8:2	9:14	6:9	8:33	7:53
SSE	10:48	6:57	8:18	7:40	7:43	7:11
MAE	10:43	6:32	9:1	7:24	7:23	7:10